Comm. Korean Math. Soc. **16** (2001), No. 3, pp. 519–541

MAGNETIC RESONANCE ELECTRICAL IMPEDANCE TOMOGRAPHY

OHIN KWON†, JIN KEUN SEO, EUNG JE WOO*, AND JEONG-ROCK YOON

ABSTRACT. Magnetic Resonance Electrical Impedance Tomography (MREIT) is a new medical imaging technique for the cross-sectional conductivity distribution of a human body using both EIT (Electrical Impedance Tomography) and MRI (Magnetic Resonance Imaging) system. MREIT system was designed to enhance EIT imaging system which has inherent low sensitivity of boundary measurements to any changes of internal tissue conductivity values. MREIT utilizes a recent CDI (Current Density Imaging) technique of measuring the internal current density by means of MRI technique. In this paper, a mathematical modeling for MREIT and image reconstruction method called the alternating J-substitution algorithm are presented. Computer simulations show that the alternating J-substitution algorithm provides accurate high-resolution conductivity images.

1. Introduction

Imaging conductivity distribution of the human body has been received considerable attention over the last 20 years, because of its potential applications in clinical fields such as tissue characterizations, plethysmography, pulmonary ventilation, stomach emptying, etc. The EIT system was used to reconstruct the internal conductivity distribution $\sigma(x, y)$ on a cross-section Ω of the human body. EIT system uses current-voltage relations on the surface of the body which are measured

Received March 8, 2000. Revised February 1, 2001.

2000 Mathematics Subject Classification: 65O99.

Key words and phrases: magnetic resonance electrical impedance tomography, current density imaging, J-substitution algorithm.

† The author was supported by the Korea Research Foundation 99-005-D0009.

* The author was supported by grant No. 2000-2-31400-008-3 from the Basic Research Program of KOSEF.

by sensing electrodes attached on the surface including the boundary $\partial\Omega$.

The principle behind the EIT system is the conductivity equation

$$\text{div}\Big(\sigma(x,y,z)\nabla u(x,y,z)\Big) = 0,$$

where u is the voltage potential. Under the assumptions that the body is cylindrical and current flows in the $xy-$plane, the three dimensional conductivity equation can be reduced to the two dimensional equation

$$\text{div}\Big(\sigma(x,y)\nabla u(x,y)\Big) = 0$$

in a slice Ω. The mathematical problem of EIT is the inverse problem of finding $\sigma(x,y)$ from the given boundary current flux $\mathbf{J}\cdot\nu|_{\partial\Omega} = \sigma\partial u/\partial\nu|_{\partial\Omega}$, where ν denotes the unit outward normal to $\partial\Omega$. Unfortunately, the boundary current flux data $\mathbf{J}\cdot\nu|_{\partial\Omega}$ used for reconstruction is not sensitive to any changes of internal tissue conductivity values, so that a small perturbation of the data $\mathbf{J}\cdot\nu|_{\partial\Omega}$ could result in a large change of σ. This highly ill-posedness makes EIT system difficult to produce true image σ with high quality.

MREIT is designed to solve many technical problems in conventional EIT. It is a new EIT imaging technique of static cross-sectional conductivity images utilizing CDI technique. The CDI technique uses MRI system to measure internal current density. Please refer to [4, 5, 6, 7] for CDI technique. In 1994, MREIT system was proposed first by Woo, Lee, and Mun[8]. However, they could not utilize the additional internal current density data effectively resulting in poor reconstruction images. Very recently, Kwon, Woo, Yoon, and Seo[1] developed a new mathematical model for MREIT where EIT system combines with CDI technique effectively. Computer simulations based on this new model provide accurate high resolution static conductivity images. Figure 1 shows the schematic diagram for MREIT system.

2. Mathematical modeling for MREIT

Let us begin with how the internal current density is obtained by means of MRI. MRI is an imaging modality based upon the nuclear magnetic resonance(NMR) signal from hydrogen atoms in the body. The intensity of a pixel in the picture of MRI is proportional to the nuclear spin density. The nuclear spin density $\rho(x,y,z)$ is obtained by NMR

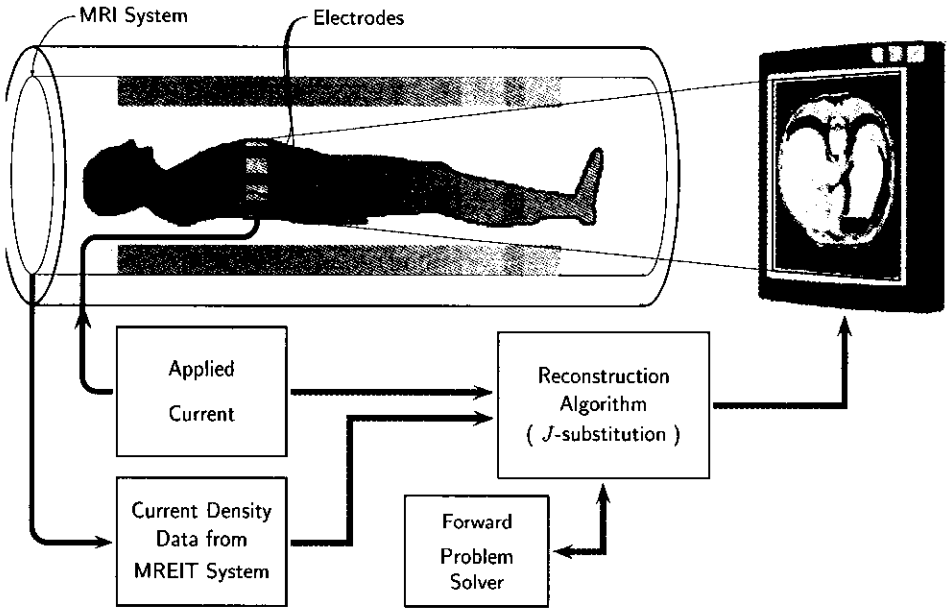

FIGURE 1. MREIT schematic diagram.

signal $S(t_x, t_y, t_z)$ in 3-dimensional data acquisition axes (t_x, t_y, t_z) using the representation formula

$$S(t_x, t_y, t_z) = \int_{\mathbb{R}^3} \rho(x, y, z) \exp[-i\gamma(xG_x t_x + yG_y t_y + zG_z t_z)]\, dxdydz,$$

where γ is the gyromagnetic ratio and G_x, G_y, G_z are the magnetic field gradient in the x, y, and z directions. We assume for a moment that the test body is a cylindrical object so that its conductivity distribution σ is a function defined on $xy-$plane. If we inject a transverse electric current independent of $z-$direction across the boundary of the cylindrical object, the induced volume current density vector $\mathbf{J}$ do not have z-component. This transverse current $\mathbf{J}$ causes a longitudinal magnetic flux density vector $\mathbf{B} = (0, 0, B_z)$. This induced magnetic field $\mathbf{B}$ with the main magnetic field $\mathbf{B}_0$ results in the new nuclear spin density ρ^* which is approximately given by

$$\rho^*(x, y, z) = \rho(x, y, z) \exp[i\gamma T_c B_z(x, y, z)],$$

where T_c is the duration of the current pulse. Therefore, by comparing two different NMR images ρ and ρ^*, we can calculate the induced

magnetic flux density strength

$$B_z(x,y,z) = \frac{1}{\gamma T_c} \tan^{-1}\left(\frac{\alpha(x,y,z)}{\beta(x,y,z)}\right), \tag{2.1}$$

where α is the imaginary part of ρ^*/ρ and β is the real part of ρ^*/ρ. This enables us to compute the internal current density from the Ampere's law

$$\mathbf{J} = \frac{1}{\mu}(\nabla \times \mathbf{B}) = \frac{1}{\mu}(\partial_y B_z, -\partial_x B_z, 0).$$

In practice, the conductivity σ of the human body is not cylindrical and the three dimensional conductivity distribution will distort the internal current density vector, so we must take the out-of-plane current into account. The $z-$component of the true current $\mathbf{J}_{\text{true}}$ will induce the transverse magnetic field B_x and B_y, the $x-$ and $y-$components of $\mathbf{B}$. However, the transverse terms B_x and B_y are relatively small compared with the longitudinal term B_z. Therefore, the calculated internal current $\mathbf{J}$ can be viewed as a small distortion of the true internal current $\mathbf{J}_{\text{true}}$.

However, this little distorted data $\mathbf{J}$ must be carefully considered in order to get accurate reconstructions with high quality image. One can develop various numerical algorithm using single current data $\mathbf{J}$, but a little distorted $\mathbf{J}$ could result in a completely different image from true one. The inevitable errors of $\mathbf{J}$ due to non-zero $x, y-$components of $\mathbf{B}$ should be reduced as much as we can.

In our MREIT system, the magnitude $|\mathbf{J}|$ will be used as a data instead of the vector $\mathbf{J}$. There are two reasons we are using this magnitude data. First, this magnitude data reduces the error, because the difference between two scalars $|\mathbf{J}_{\text{true}}|$ and $|\mathbf{J}|$ is smaller than the distance between two vectors $\mathbf{J}_{\text{true}}$ and $\mathbf{J}$. Second, it has been proved that two different internal currents are required to reconstruct σ accurately. For one current, a little distorted data $\mathbf{J}$ could lead to a completely different conductivity image from the true one (See [2] for details). The two currents $\mathbf{J}_1$ and $\mathbf{J}_2$ have the unique connection by the relation

$$\frac{|\mathbf{J}_1|}{|\nabla u_1|} = \frac{|\mathbf{J}_2|}{|\nabla u_2|}$$

due to the fact that the conductivity is unchanged under different currents. Here, u_j is the corresponding voltage potential to $\mathbf{J}_j$, $j = 1, 2$. In order to connect two different conductivity equations, it is more convenient for us to use the magnitude $|\mathbf{J}|$ as a data for MREIT system. We will discuss this connection later.

Now, we are ready to explain the mathematical model for MREIT explicitly. Let Ω be a cross-section of the body. For an applied current g on the boundary $\partial\Omega$, the electric potential u can be viewed as a weak solution in the sobolev space $H^1(\Omega)$ of the Neumann problem

$$\operatorname{div}\Big(\sigma(x,y)\nabla u(x,y)\Big) = 0 \quad \text{in } \Omega,$$
$$\sigma\frac{\partial u}{\partial \nu} = g \quad \text{on } \partial\Omega, \quad \text{and} \int_{\partial\Omega} u\,ds = 0,$$

where ν denotes the outward unit normal vector to $\partial\Omega$. However, we cannot solve this standard Neumann problem because σ is unknown. Our MREIT model utilizes the additional data $a(x,y) = |\mathbf{J}(x,y)|$ which is obtained by CDI technique. So, we can remove the unknown variable σ in the conductivity equation by replacing the division of the magnitude of the internal current density by the magnitude of the electric field. Then the electric potential u becomes a solution of the nonlinear partial differential equation

$$\begin{aligned} &\operatorname{div}\left(\frac{a(x,y)}{|\nabla u(x,y)|}\nabla u(x,y)\right) = 0 \quad \text{in } \Omega, \\ &\frac{a}{|\nabla u|}\frac{\partial u}{\partial \nu} = g \quad \text{on } \partial\Omega, \quad \text{and} \int_{\partial\Omega} u\,ds = 0. \end{aligned} \tag{2.2}$$

It seems that, using the additional information on the internal current density, the highly ill-posed inverse conductivity problem is changed into the forward nonlinear problem (2.2). So, it is natural to consider the major classical questions for the forward problem (2.2) such as existence, uniqueness, and regularity properties. Unfortunately, the problem (2.2) has several examples of non-existence and non-uniqueness. In our practical study, the existence question could be ignored, but the issue of uniqueness must be seriously concerned, because it is related to the uniqueness of the conductivity image. Hence, the model equation (2.2) must be revised to guarantee the uniqueness.

Notice that the equation (2.2) should not be regarded as the limit of the similar equations

$$\operatorname{div}\Big(a(x,y)|\nabla u(x,y)|^{p-2}\nabla u(x,y)\Big) = 0 \qquad \text{as } p \to 1$$

or

$$\operatorname{div}\left(\frac{a(x,y)}{\sqrt{\epsilon^2 + |\nabla u(x,y)|^2}}\nabla u(x,y)\right) \qquad \text{as } \epsilon \to 0$$

because the limiting solutions could be far different from the seeking solution. We should not go astray from the main point.

If a revised model has uniqueness, the unique solution must agree with the practical solution. To revise the model (2.2), we need look into how current flows on the interface of conductivity change. For considering a simple conducting material consisting of two homogeneous media with different conductivities, the normal component of the current density $\mathbf{J}$ is continuous across the interface while its tangential components change. Therefore, if $\mathbf{J}$ is orthogonal to the level curve of σ, the datum $a = \sigma|\nabla u|$ does not contain any information of the variation of σ. To draw the level curve of σ, it is important to note that the direction ∇u on the level curve of σ should not be pointing at the normal direction (for more details, see section 3 and 4). From this reason, the alternating J-substitution algorithm uses two applied currents g_1 and g_2 so that the corresponding electric fields ∇u_1 and ∇u_2 point at two different directions satisfying $\nabla u_1 \times \nabla u_2 \neq 0$ in the domain Ω. Since the conductivity σ will be unchanged with different injected currents, it must be

$$\frac{a_1(x,y)}{|\nabla u_1(x,y)|} = \frac{a_2(x,y)}{|\nabla u_2(x,y)|} \quad \text{in } \Omega,$$

where a_1 and a_2 are the magnitude of current density corresponding to g_1 and g_2, respectively. Thus, we derive the following revised model

$$\begin{aligned}
&\operatorname{div}\left(\frac{a_2(x,y)}{|\nabla u_2(x,y)|}\nabla u_1(x,y)\right) = 0 \quad \text{in } \Omega,\\
&\operatorname{div}\left(\frac{a_1(x,y)}{|\nabla u_1(x,y)|}\nabla u_2(x,y)\right) = 0 \quad \text{in } \Omega,\\
&\frac{a_2}{|\nabla u_2|}\frac{\partial u_1}{\partial \nu} = g_1 \ \text{ and } \ \frac{a_1}{|\nabla u_1|}\frac{\partial u_2}{\partial \nu} = g_2 \quad \text{on } \partial\Omega,\\
&\frac{a_1(x,y)}{|\nabla u_1(x,y)|} = \frac{a_2(x,y)}{|\nabla u_2(x,y)|} \quad \text{in } \Omega,\\
&\int_{\partial\Omega} u_1\, ds = \int_{\partial\Omega} u_2\, ds = 0.
\end{aligned} \tag{2.3}$$

To apply two Neumann data g_1 and g_2 in our real MREIT system, four electrodes are placed at four sides of $\partial\Omega$, so that two different currents flow using two pairs of electrodes (See Figure 2 (a)). Figure 2 (b) shows that B_z component for the phantom in Figure 2 (a) calculated from the nuclear spin densities ρ^* and ρ in (2.1). Based on the mathematical model (2.3) for the MREIT system, we could develop an accurate reconstruction algorithm, so called the alternating J-substitution algorithm. In the alternating J-substitution algorithm, the conductivity σ is reconstructed iteratively by means of two measurements as follows.

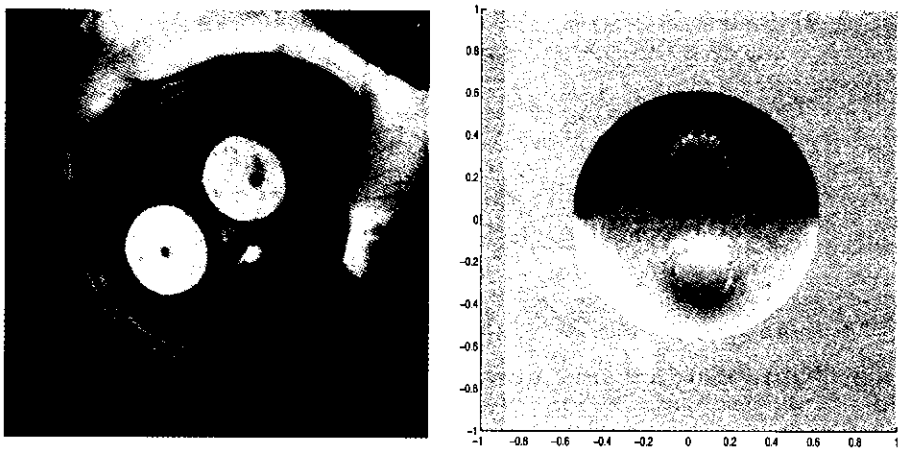

(a) (b)

FIGURE 2. (a) A phantom for MREIT system, (b) The z-component of magnetic flux $\mathbf{B}$

Alternating J-substitution Algorithm

(1) *Initial guess* : For an initial guess, we may choose a homogeneous conductivity σ_0, for example, $\sigma_0 \equiv 1$. Let $n = 0$.

(2) *Forward solver with respect to* g_1 : For a given conductivity σ_n, we solve the forward problem given by

$$\operatorname{div}(\sigma_n \nabla u_1^n) = 0 \quad \text{in } \Omega,$$

$$\sigma_n \frac{\partial u_1^n}{\partial \nu} = g_1 \quad \text{on } \partial\Omega \quad \text{and} \quad \int_{\partial\Omega} u_1^n \, ds = 0.$$

(3) *Updating strategy with respect to* g_1 : Update the conductivity in the next step by

$$\sigma_{n+1/2} := \frac{a_1}{|\nabla u_1^n|} \quad \text{in } \Omega.$$

(4) *Forward solver with respect to* g_2 : For a given conductivity $\sigma_{n+1/2}$, we solve the forward problem given by

$$\operatorname{div}\left(\sigma_{n+1/2} \nabla u_2^{n+1/2}\right) = 0 \quad \text{in } \Omega,$$

$$\sigma_{n+1/2} \frac{\partial u_2^{n+1/2}}{\partial \nu} = g_2 \quad \text{on } \partial\Omega \quad \text{and} \quad \int_{\partial\Omega} u_2^{n+1/2} \, ds = 0.$$

(5) *Updating strategy with respect to* g_2 : Update the conductivity in the next step by

$$\sigma_{n+1} := \frac{a_2}{|\nabla u_2^{n+1/2}|} \quad \text{in } \Omega.$$

(6) *Stopping rule* : If $|\sigma_{n+1} - \sigma_n| < \epsilon$ for some measurement precision ϵ, stop; otherwise go back to step (2) substituting $n \leftarrow n+1$.

3. Non-existence and non-uniqueness

In this section, we discuss the existence and uniqueness for the nonlinear Neumann boundary value problem

$$\begin{aligned} &\operatorname{div}\left(\frac{a(x,y)}{|\nabla u(x,y)|}\nabla u(x,y)\right) = 0 \quad \text{in } \Omega, \\ &\frac{a}{|\nabla u|}\frac{\partial u}{\partial \nu} = g \quad \text{on } \partial\Omega, \quad \text{and} \int_{\partial\Omega} u\, ds = 0. \end{aligned} \tag{3.1}$$

When $a \equiv 1$, the nonlinear forward problem (3.1) is reduced to p-Laplace equation

$$\operatorname{div}(|\nabla u|^{p-2}\nabla u) = 0 \quad \text{for } p = 1.$$

But 1-Laplace equation has quite different nature from p-Laplace equation for $1 < p < \infty$. Indeed, most properties in p-Laplace equation for $1 < p < \infty$ may not hold for 1-Laplace equation.

For simplicity, we confine ourselves to a unit square domain $\Omega = (0,1) \times (0,1)$ in $\mathbb{R}^2$. We assume $a \geq 0$ is a piecewise $\mathcal{C}^2$ function and $g \in L_0^2(\partial\Omega) = \{L^2(\partial\Omega) \mid \int_{\partial\Omega} g\, ds = 0\}$. As a simple example, let us consider weak solutions of 1-Laplace equation with the injected current g on $\partial\Omega$ given by

$$g(x,y) = \begin{cases} -1 & \text{if } x = 0, \\ 1 & \text{if } x = 1, \\ 0 & \text{otherwise.} \end{cases} \tag{3.2}$$

This example has infinitely many weak solutions. To be precise, let us introduce a function of the form

$$u_\phi(x,y) = \left(x - \frac{1}{2}\right) + \phi(x),$$

where $\phi(x)$ is a compactly supported function in the interval $(0,1)$ such that

(3.3)

$$\phi \in H^1(0,1), \quad \int_0^1 \phi(x)\,dx = 0, \quad -1 < \phi'(x) < \infty \text{ for almost all } x \in (0,1).$$

It is easy to see that this u_ϕ is the weak solution of the elliptic Neumann boundary problem

$$\operatorname{div}\left(\frac{1}{1+\phi'(x)}\nabla u_\phi(x,y)\right) = 0 \quad \text{in } \Omega,$$

$$\frac{1}{1+\phi'}\frac{\partial u_\phi}{\partial \nu} = g \quad \text{on } \partial\Omega, \quad \text{and} \quad \int_{\partial\Omega} u_\phi\,ds = 0.$$

Hence any u_ϕ, where ϕ satisfies (3.3), solve the same nonlinear equation (3.1) with $a \equiv 1$ and the Neumann data (3.2). This non-uniqueness tells us that the reconstruction of the conductivity from a single equation (3.1) may be impossible, because two different solutions u_{ϕ_1} and u_{ϕ_2} of (3.1) give two different conductivity images

$$\sigma_1 = \frac{1}{1+\phi_1'(x)} \quad \text{and} \quad \sigma_2 = \frac{1}{1+\phi_2'(x)}.$$

To discuss the non-existence question, first let us consider one dimensional case

$$\left(\frac{a(t)}{|u'(t)|}u'(t)\right)' = 0 \quad \text{in } (0,1).$$

Since $u'(t)/|u'(t)|$ is either 1 or -1, it must be that $a'(t) = 0$ almost everywhere. The corresponding result in two dimensional case is as follow.

THEOREM 3.1. *Let $\Omega = (0,1)\times(0,1)$ and $g \in L_0^2(\partial\Omega)$ be given by (3.2). Assume that $a(x,y)$ is a positive C^1 function such that $\partial a/\partial y = 0$. Then the necessary condition for the existence of solutions in $C^1(\Omega)$ of the nonlinear problem (3.1) is that $a \equiv 1$ in Ω.*

PROOF. We will only prove that $a \geq 1$ and please refer to [2] for the proof of $a \leq 1$. For an arbitrarily chosen $t \in (0,1)$ and $h > 0$, define a function

$$\eta_{t,h}(x,y) = \begin{cases} 0 & \text{if } 0 < x < t, \\ \dfrac{1}{h}(x-t) & \text{if } t < x < t+h, \\ 1 & \text{if } t+h < x < 1. \end{cases}$$

Applying $\eta_{t,h}$ as a test function to the Neumann problem (3.1), with the help of (3.2) we obtain

$$\frac{1}{h}\int_t^{t+h} a(x)\,dx \le \frac{1}{h}\int_t^{t+h} a(x)\left\{\int_0^1 \frac{1}{|\nabla u|}\frac{\partial u}{\partial x}dy\right\}dx = 1,$$

because $\partial_x u/|\nabla u| \le 1$. Since h is arbitrarily small, it must be $a(t) \ge 1$ for any $t \in (0,1)$. □

This counter example indicates that a single pair of data (g,a) is not sufficient to reconstruct the conductivity. This is the reason why we require at least two different pairs (g_1,a_1) and (g_2,a_2) for the uniqueness of the inverse problem to reconstruct the conductivity distribution, which will be discussed in the following section.

4. Uniqueness of the inverse problem with two measurements

As discussed in the previous section, one measurement is not enough to determine σ uniquely. Therefore in this section, we consider the decoupled revised model motivated from (2.3) utilizing two measurements.

$$\begin{aligned}
&\operatorname{div}\left(\frac{a_1(x,y)}{|\nabla u_1(x,y)|}\nabla u_1(x,y)\right) = 0 \quad \text{in } \Omega,\\
&\operatorname{div}\left(\frac{a_2(x,y)}{|\nabla u_2(x,y)|}\nabla u_2(x,y)\right) = 0 \quad \text{in } \Omega,\\
&\frac{a_1}{|\nabla u_1|}\frac{\partial u_1}{\partial \nu} = g_1 \ \text{ and } \ \frac{a_2}{|\nabla u_2|}\frac{\partial u_2}{\partial \nu} = g_2 \quad \text{on } \partial\Omega,\\
&\frac{a_1(x,y)}{|\nabla u_1(x,y)|} = \frac{a_2(x,y)}{|\nabla u_2(x,y)|} \quad \text{in } \Omega,\\
&\int_{\partial\Omega} u_1\,ds = \int_{\partial\Omega} u_2\,ds = 0.
\end{aligned} \tag{4.1}$$

In the human body, the conductivity distribution can be viewed as a piecewise continuous function contained in the following class

$$\Sigma := \Big\{\sigma = \sigma_0 + \sum_{i=1}^{M} \sigma_i \chi_{D_i} \,\Big|\, \sigma_0, \sigma_i \in C^{\alpha}(\bar{\Omega}) \text{ for some } 0 < \alpha < 1,\ M \in \mathbb{N},$$
$$D_i \subset\subset \Omega \text{ with } C^{1,\alpha} \text{ boundary, which satisfies } \bar{D}_i \cap \bar{D}_j = \emptyset$$
$$\text{for } i \neq j, \text{ and } \sigma_i > 0 \text{ or } \sigma_i < 0 \text{ on } \bar{D}_i,\ \sigma_L \leq \sigma \leq \sigma_U \text{ for some}$$
$$\text{constants } \sigma_L, \sigma_U > 0\Big\}.$$

So, our aim is turned into finding the unknown inclusion

$$D = \bigcup_{i=1}^{M} D_i$$

by solving the MREIT model expressed by (2.3) or (4.1). First, we need to choose the appropriate pair of current patterns g_1 and g_2 so that the corresponding voltage potentials u_1 and u_2 satisfy $\nabla u_1(x,y) \times \nabla u_2(x,y) = 0$ for all $(x,y) \in \Omega$. This requires some technical definition for the currents g. A function $g \in L_0^2(\partial\Omega)$ is said to *have only one sign change on* $\partial\Omega$, if there exists a pair of connected subsets $(\partial\Omega^+, \partial\Omega^-)$ of $\partial\Omega$ such that

$$\partial\Omega^+ \cup \partial\Omega^- = \partial\Omega, \quad \partial\Omega^+ \cap \partial\Omega^- = \emptyset,$$

and

$$g \geq 0 \text{ on } \partial\Omega^+, \quad g \leq 0 \text{ on } \partial\Omega^-.$$

For example, the function $c_1 g_1 + c_2 g_2$ has only one sign change for arbitrary nonzero vector $(c_1, c_2) \in \mathbb{R}^2$, where g_1 and g_2 are defined by

$$g_1(x,y) = \begin{cases} -1 & \text{if } 1/2 - \epsilon \leq y \leq 1/2 + \epsilon \text{ and } x = 0, \\ 1 & \text{if } 1/2 - \epsilon \leq y \leq 1/2 + \epsilon \text{ and } x = 1, \\ 0 & \text{otherwise,} \end{cases}$$

(4.2)

$$g_2(x,y) = \begin{cases} -1 & \text{if } 1/2 - \epsilon \leq x \leq 1/2 + \epsilon \text{ and } y = 0, \\ 1 & \text{if } 1/2 - \epsilon \leq x \leq 1/2 + \epsilon \text{ and} y = 1, \\ 0 & \text{otherwise,} \end{cases}$$

for some $0 < \epsilon \leq 1/2$. This example includes the current patterns that are used to reconstruct the actual conductivity distribution in [1]. The following observation plays an important role in the process of the proof of our main theorems.

LEMMA 4.1. *Let g_1, $g_2 \in L_0^2(\partial\Omega)$ be given so that $c_1 g_1 + c_2 g_2$ has only one sign change on $\partial\Omega$ for any nonzero vector $(c_1, c_2) \in \mathbb{R}^2$. If there exist solutions $u_j \in H^1(\Omega)$ to the nonlinear problems*

$$\begin{aligned} &\operatorname{div}\left(\frac{a_j(x)}{|\nabla u_j(x)|}\nabla u_j(x)\right) = 0 \quad \text{in} \quad \Omega, \\ &\frac{a_j}{|\nabla u_j|}\frac{\partial u_j}{\partial \nu} = g_j \quad \text{on} \quad \partial\Omega, \quad \text{and} \quad \int_{\partial\Omega} u_j \, ds = 0 \end{aligned} \tag{4.3}$$

for $j = 1, 2$, and the solutions satisfy a priori condition

$$\frac{a_1}{|\nabla u_1|} = \frac{a_2}{|\nabla u_2|},$$

then we have

$$c_1 \nabla u_1(x) + c_2 \nabla u_2(x) \neq 0$$

for all $x \in \Omega$ and nonzero vector $(c_1, c_2) \in \mathbb{R}^2$.

PROOF. For the proof, see [2]. □

Lemma 4.1 tells us that two gradient vector fields ∇u_1 and ∇u_2 never vanish, and moreover, these vectors are never parallel at any points under the described assumptions. Using this fact, we can prove the following uniqueness result for the inverse problem with two measurements.

THEOREM 4.2. *Let g_1, $g_2 \in L_0^2(\partial\Omega)$ satisfy the same assumption in Lemma 4.1. If there exist solutions $u_j \in H^1(\Omega)$ to the nonlinear problems* (4.3) *for $j = 1, 2$, and*

$$\frac{a_1}{|\nabla u_1|} = \frac{a_2}{|\nabla u_2|}$$

is assumed to be represented by a function

$$\sigma = \sigma_0 + \sum_{i=1}^{M} \sigma_i \chi_{D_i} \in \Sigma.$$

Then the unknown inclusion $D = \bigcup_{i=1}^{M} D_i$ is reconstructed by the measured data (a_1, a_2) such that

$$\partial D = \{x \in \Omega \,|\, a_1 \text{ or } a_2 \text{ is discontinuous at } x\}.$$

PROOF. For the proof, see [2]. □

Theorem 4.2 shows that under the prescribed assumptions the region where the conductivity distribution has jumps can be detected by the observation of the discontinuities of the measured data (a_1, a_2). In the following theorem, we show that the conductivity values as well as the unknown inclusions can be determined in a simple case when we know that the conductivity distribution $\sigma \in \Sigma$ is known to be piecewise constants.

THEOREM 4.3. *Under the same assumptions in Theorem 4.2 with an additional assumption that*

$$\frac{a_1}{|\nabla u_1|} = \frac{a_2}{|\nabla u_2|}$$

is supposed to be represented by a function

$$\sigma = 1 + \sum_{i=1}^{M} \mu_i \chi_{D_i} \in \Sigma \quad \text{for some } M \in \mathbb{N},$$

where μ_i is a constant with $0 \neq \mu_i \in (-1, \infty)$ for all $i = 1, \cdots, M$, the conductivity distribution σ is thoroughly determined by the measured data (a_1, a_2).

PROOF. For the proof, see [2]. □

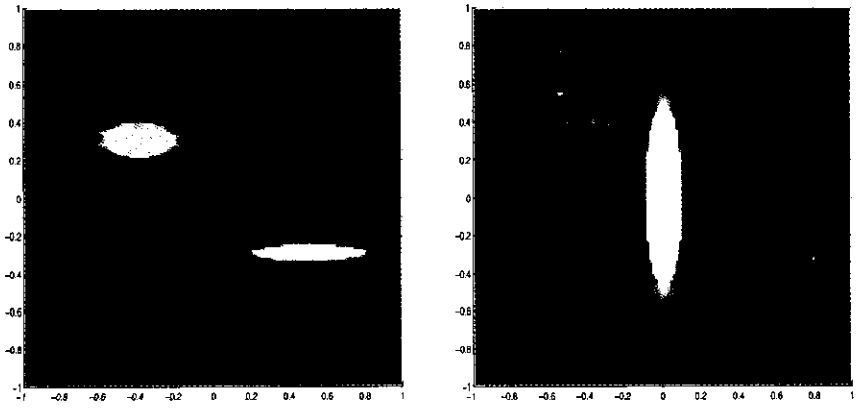

$a_1(x, y)$ $a_2(x, y)$

FIGURE 3. The current densities a_1 and a_2 corresponding to the current pattern g_1 and g_2 described in (4.2) with $\epsilon = 1/2$, respectively.

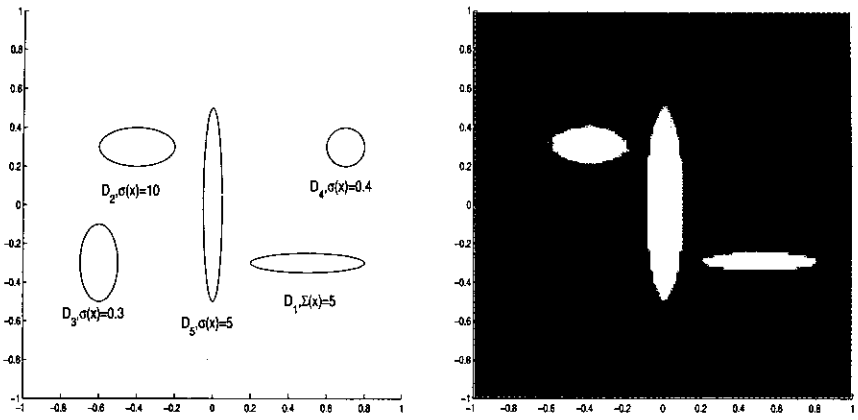

FIGURE 4. The target to be reconstructed and the image of the sum of current densities.

To show the feasibility of the result in Theorem 4.2 and 4.3, we tested a numerical reconstruction. The test model is taken with multiple anomalies $D = \cup_{j=1}^{5} D_j$, the boundaries of which are parametrically represented and the conductivity values are given as follows.

$$\begin{aligned}
\partial D_1 &= \{(0.5 + 0.3\cos\theta, -0.3 + 0.05\sin\theta) \,|\, \theta \in [0, 2\pi)\}, \quad \sigma = 5 \quad \text{in } D_1,\\
\partial D_2 &= \{(-0.4 + 0.2\cos\theta, 0.3 + 0.1\sin\theta) \,|\, \theta \in [0, 2\pi)\}, \quad \sigma = 10 \quad \text{in } D_2,\\
\partial D_3 &= \{(-0.6 + 0.1\cos\theta, -0.3 + 0.2\sin\theta) \,|\, \theta \in [0, 2\pi)\}, \quad \sigma = 0.3 \quad \text{in } D_3,\\
\partial D_4 &= \{(0.7 + 0.1\cos\theta, 0.3 + 0.1\sin\theta) \,|\, \theta \in [0, 2\pi)\}, \quad \sigma = 0.4 \quad \text{in } D_4,\\
\partial D_5 &= \{(0.05\cos\theta, 0.5\sin\theta) \,|\, \theta \in [0, 2\pi)\}, \quad \sigma = 5 \quad \text{in } D_5.
\end{aligned}$$

Figure 3 shows the internal current densities $a_1(x, y)$ and $a_2(x, y)$ corresponding to the current pattern g_1 and g_2 described in (4.2) with $\epsilon = 1/2$, respectively. With these data, the image constructed from the sum of a_1 and a_2 is presented in Figure 4 in comparison with the target image. The discontinuous region in the summed image corresponds to the boundaries to be detected by virtue of Theorem 4.2, and from the ratio of discontinuities we can calculate the conductivity values by virtue of Theorem 4.3, the precise formula of which can be found in [2].

5. Alternating J-substitution algorithm

The alternating J-substitution algorithm makes use of two data which are the magnitude of internal current density induced by Neumann data

g_1 and g_2 in (4.2). Then the MREIT image reconstruction becomes the iterative algorithm to update $\sigma = a/|\nabla u|$, which is summarized at the end of section 2. In the paper [3], we obtained a pseudo-convergence result on the *alternating J-substitution algorithm.*

THEOREM 5.1. (Pseudo Convergence) *Let u_1^n and $u_2^{n+1/2}$ be the iterative solutions with respect to the Neumann data g_1 and g_2 belonging to $L_0^2(\partial\Omega)$, respectively. Then we have*

$$\begin{aligned}
&\int_\Omega (\sigma_{n+1} - \sigma) \left\{ \left(1 + \frac{\sigma_{n+1}}{\sigma}\right) \frac{a_2^2}{\sigma_{n+1}^2} \right\} dx \\
= &\int_\Omega (\sigma_{n+1/2} - \sigma) \left\{ \left(1 + \frac{\sigma_{n+1}}{\sigma}\right) \frac{a_2^2}{\sigma_{n+1}^2} \right\} \\
&\times \left\{ \frac{|\nabla u_2^{n+1/2} \cdot (\nabla u_2^{n+1/2} + \nabla u_2)|}{|\nabla u_2^{n+1/2}|(|\nabla u_2^{n+1/2}| + |\nabla u_2|)} \right\} dx
\end{aligned}$$

and

$$\begin{aligned}
&\int_\Omega (\sigma_{n+1/2} - \sigma) \left\{ \left(1 + \frac{\sigma_{n+1/2}}{\sigma}\right) \frac{a_1^2}{\sigma_{n+1/2}^2} \right\} dx \\
= &\int_\Omega (\sigma_n - \sigma) \left\{ \left(1 + \frac{\sigma_{n+1/2}}{\sigma}\right) \frac{a_1^2}{\sigma_{n+1/2}^2} \right\} \left\{ \frac{|\nabla u_1^n \cdot (\nabla u_1^n + \nabla u_1)|}{|\nabla u_1^n|(|\nabla u_1^n| + |\nabla u_1|)} \right\} dx.
\end{aligned}$$

PROOF. For the proof, see [3]. □

Now we turn our attention to the discretized problem. For simplicity, let $\Omega = (-1,1) \times (-1,1)$. In practice, the MR image consists of $N \times N$ pixel values, so that the data a is also given by a constant value on each pixel. So, we divide Ω into an assembly of pixels in such a way that

$$\bar{\Omega} = \bigcup_{k=0}^{N-1} \bar{\Omega}_k, \quad \Omega_i \cap \Omega_j = \emptyset \quad \text{if } i \neq j,$$

where Ω_k are uniformly axis-parallel sub-rectangular elements that correspond to pixels. We imply a standard cell centered finite difference

scheme as a technique for constructing approximate solution for the forward problem

$$\begin{aligned} &\operatorname{div}(\sigma\nabla u)) = 0 \quad \text{in } \Omega, \\ &\sigma\frac{\partial u}{\partial \nu} = g \quad \text{on } \partial\Omega, \quad \text{and} \quad \int_{\partial\Omega} u\, ds = 0. \end{aligned} \tag{5.1}$$

We assume that the conductivity in each element is homogeneous, that is,

$$\sigma = \sum_{k=0}^{N^2-1} \sigma_k \chi_{\Omega_k},$$

where σ_k is a positive constant.

5.1. Cell-centered finite difference method

Let the center of the cell Ω_{i+jN} be denoted by (x_i, y_j). Since u satisfies Laplace equation on each pixel Ω_k,

$$\int_{\partial\Omega_k} \frac{\partial u}{\partial \nu}\, ds = 0, \quad 0 \le k \le N^2 - 1,$$

and therefore we obtain the following approximation for $1 \le i, j \le N-2$

$$\begin{aligned} &\left\{ \frac{\partial u((x_i + x_{i+1})/2, y_j)}{\partial x} - \frac{\partial u((x_i + x_{i-1})/2, y_j)}{\partial x} \right. \\ &\left. + \frac{\partial u(x_i, (y_j + y_{j+1})/2)}{\partial y} - \frac{\partial u(x_i, (y_j + y_{j-1})/2)}{\partial y} \right\} \approx 0. \end{aligned} \tag{5.2}$$

The interface condition between Ω_{i+jN} and Ω_{i+1+jN} can be understood approximately

$$\begin{aligned} &\sigma_{i+jN}\Big(u((x_i + x_{i+1})/2, y_j) - u(x_i, y_j)\Big) \\ &\approx \sigma_{i+1+jN}\Big(u(x_{i+1}, y_j) - u((x_i + x_{i+1})/2, y_j)\Big) \end{aligned}$$

and this implies

$$u((x_i + x_{i+1})/2, y_j) \approx \frac{\sigma_{i+jN} u(x_i, y_j) + \sigma_{i+1+jN} u(x_{i+1}, y_j)}{\sigma_{i+jN} + \sigma_{i+1+jN}}. \tag{5.3}$$

By using the approximation (5.3), we obtain

$$(5.4)\quad \frac{\partial u((x_i+x_{i+1})/2, y_j)}{\partial x} \approx \frac{u((x_i+x_{i+1})/2, y_j) - u(x_i, y_j)}{h/2} \approx \frac{2\sigma_{i+1+jN}(u(x_{i+1}, y_j) - u(x_i, y_j))}{h(\sigma_{i+jN} + \sigma_{i+1+jN})}.$$

By substituting the relation (5.4) and similar approximations into (5.2), the forward problem (5.1) is converted into the linear system

$$(5.5)\quad \mathbf{A}u^N = \mathbf{b}_N,$$

where $\mathbf{A}$ is $N^2 \times N^2$ matrix and $\mathbf{b}_N$ is generated by the Neumann data g.

5.2. Multi-level J-substitution algorithm

The number N^2 is the total number of pixels of MR images (usually $N = 128$, or 256). If $N = 256$, the size of the admittance matrix $\mathbf{A}$ is 65536×65536. For this large size matrix, it is essential to solve the forward problem efficiently and reduce the iteration numbers until an appropriate stopping criterion is satisfied.

In this paper, we consider the *multi-level J-substitution algorithm* in which the main strategy is to incorporate the idea of using coarse grids to obtain better initial guesses. Let us denote by Ω^h the net domain of Ω with the pixel size h. For using coarse grid correction, define the transfer operators I_{2h}^h and I_h^{2h} which are called interpolation and restriction operators, respectively. We use two applied currents g_1 and g_2, and denote the corresponding magnitude of current densities by a_1^h and a_2^h, respectively.

Multi-level J-substitution Algorithm

(1) Apply the restriction operator I_h^{2h} recursively to the current density a_i^h, $i = 1, 2$, which are given data from MRI system with $N \times N$ components and obtain reduced vectors a_i^{mh} on a coarse grid Ω^{mh} for a fixed number m.
   (a) For the initial guess, choose a homogeneous conductivity $\sigma_0 \equiv 1$.
   (b) For given σ_n, find u_i^n which is the numerical solution on the domain Ω^{mh} with applied current g_i and conductivity σ_n.

(c) Update σ_{n+1} as in J-substitution procedure

$$\sigma_{n+1/2} = \frac{a_1^{mh}}{|\nabla u_1^n|}, \quad \sigma_{n+1} = \frac{a_2^{mh}}{|\nabla u_2^{n+1/2}|}.$$

(d) If $|\sigma_{n+1} - \sigma_n| < \epsilon$ for some measurement precision ϵ, stop; otherwise go back to step (b).

(2) $\Omega^{mh} \to \Omega^{(m-1)h}$: take the conductivity initial guess by applying the interpolation operator $I_{mh}^{(m-1)h}$ to the iterative conductivity solution $\tilde{\sigma}$ on the grid Ω^{mh}. Perform the iterative steps (b) to (d). Proceed inductively to reach the original grid Ω^h.

6. Numerical experiments

Let the test domain be $\Omega = (-1,1) \times (-1,1)$ and the current data g_1 and g_2 on $\partial\Omega$ be given by

$$g_1(x,y) = \begin{cases} -1 & \text{if } |y| \le 0.05 \text{ and } x = -1, \\ 1 & \text{if } |y| \le 0.05 \text{ and } x = 1, \\ 0 & \text{otherwise,} \end{cases}$$

$$g_2(x,y) = \begin{cases} -1 & \text{if } |x| \le 0.05 \text{ and } y = -1, \\ 1 & \text{if } |x| \le 0.05 \text{ and } y = 1, \\ 0 & \text{otherwise.} \end{cases} \tag{6.1}$$

6.1. Toy model

It consists of four anomalies in which the relative resistivities with respect to background are 0.25 in the white disk, 2 in two grey trapezoids, and 5 in the dark ring (see Figure 5).

For practical implementations, internal current densities $a_1(x,y)$ and $a_2(x,y)$ (Figure 5) are assumed to be observation data from MRI system which are artificially corrupted by adding 3% random noise to the computed current density distributions $b_1(x)$ and $b_2(x)$ obtained by solving the linear system (5.5);

$$a_i(x,y) = (1 + 0.03 * rand\_number(x,y))b_i(x,y), \quad (x,y) \in \Omega, \ i = 1,2,$$

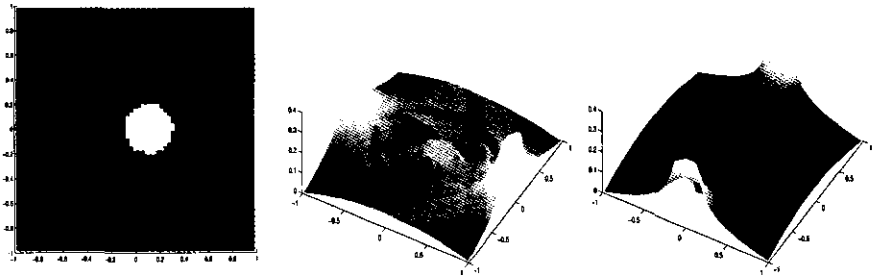

FIGURE 5. The target to be reconstructed in toy model and current density images a_1 and a_2 corresponding to g_1 and g_2 described in (6.1), respectively.

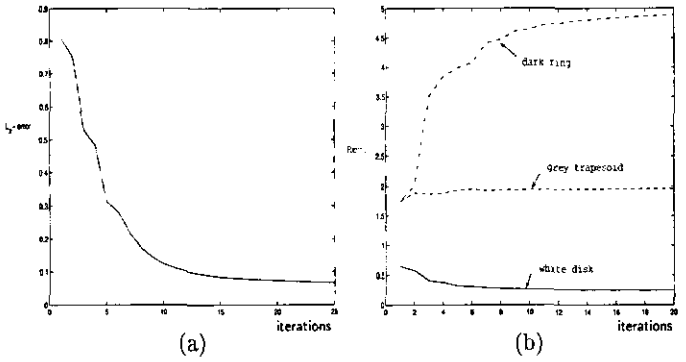

FIGURE 6. (a) The relative L^2-error and (b) Convergence behavior of conductivity value on each anomaly.

where $rand\_number(x,y)$ is a uniformly distributed random number generator in $(-1,1)$. In this example, we take a standard conjugate gradient method to solve (5.5) and assume 64×64 pixel values. The relative L^2-error defined by $\mathcal{E}_n := \| \sigma - \sigma_n \| / \| \sigma \|$, where σ_n denotes the conductivity distribution at n-th iteration and σ is the target conductivity distribution. Figure 6 (a) plots the relative L^2-error. Figure 6 (b) shows the improvement of conductivity values on each anomaly as a function of iteration number.

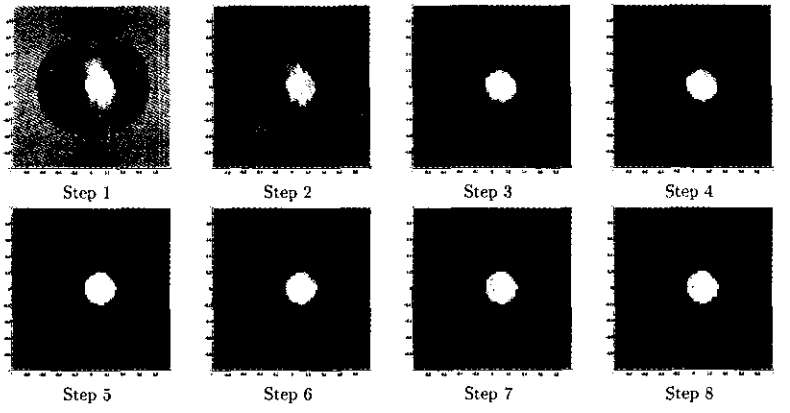

FIGURE 7. Updated conductivity images.

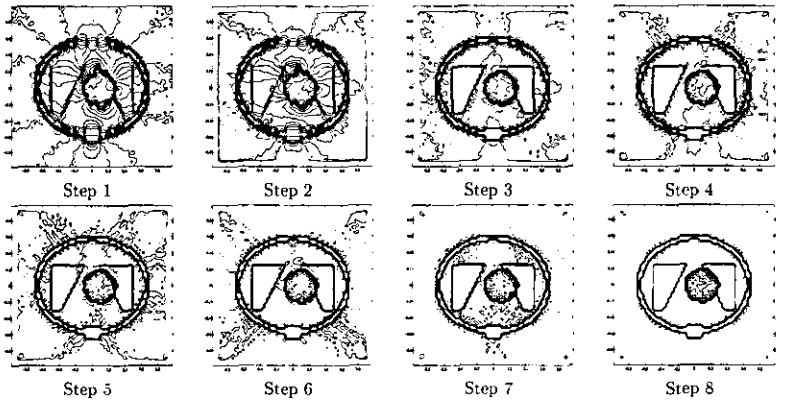

FIGURE 8. Updated conductivity images (Contour plot).

Figure 7 shows the updated conductivity image for each step by using *alternating J-substitution algorithm* and Figures 8 shows the contour lines for each updated conductivity image.

6.2. Realistic model

We test a more complicated model, which is based on a real MR image (see Figure 10), in order to show the feasibility of *alternating J-substitution algorithm*. We take 256×256 mesh grid in this numerical experiment, so it is important to use an efficient forward solver. Figures

9 presents the current densities corresponding to the current pattern g_1 and g_2 given in (6.1), respectively.

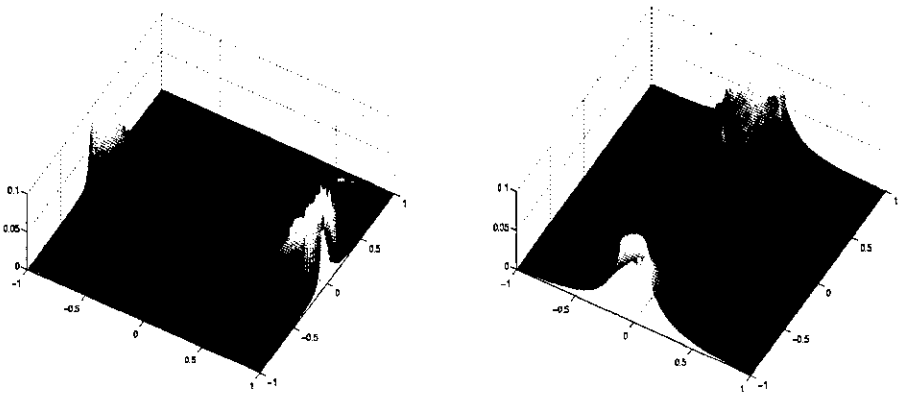

$a_1(x, y)$ $a_2(x, y)$

FIGURE 9. Current density images a_1 and a_2 corresponding to g_1 and g_2 described in (6.1), respectively.

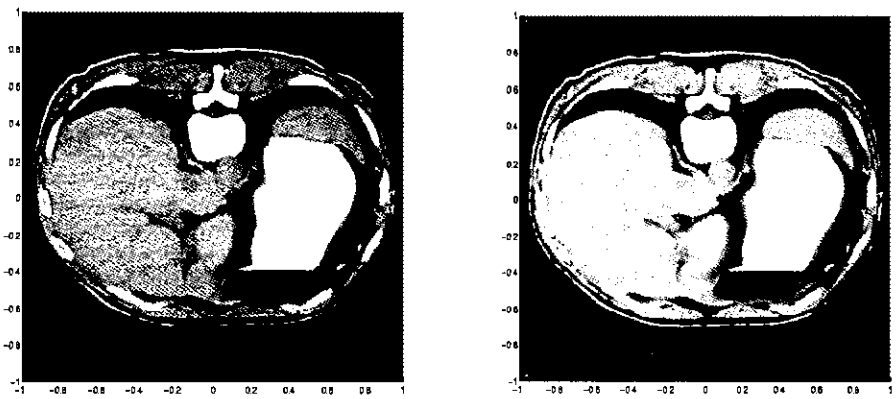

Target Reconstructed

FIGURE 10. Target conductivity image and the reconstructed image using the alternating J-substitution algorithm.

Figure 10 shows the reconstructed conductivity image in comparison with the target conductivity image.

References

[1] O. Kwon, E. J. Woo, J. R. Yoon, and J. K. Seo, *Magnetic Resonance Electrical Impedance Tomography (MREIT) : Simulation Study of J-Substitution Algorithm*, submitted for publication.

[2] S. W. Kim, O. Kwon, J. K. Seo, and J. R. Yoon, *On a nonlinear partial differential equation arising in MREIT*, in preparation.

[3] O. Kwon, J. K. Seo, and J. R. Yoon, *Alternating J-substitution algorithm and its convergence analysis for MREIT*, in preparation.

[4] H. R. Gamba and D. T. Delpy, *Measurement of electrical current density distribution within the tissues of the head by magnetic resonance imaging*, Med. Biol. Eng. Comp. **36** (1998), 165–170.

[5] G. C. Scott, M. L. G. Joy, R. L. Armstrong, and R. M. Henkelman, *Measurement of nonuniform current density by magnetic resonance*, IEEE Trans. Med. Imag. **10** (1991), 362–374.

[6] ———, *Sensitivity of magnetic-resonance current density imaging*, J. Mag. Res. **97** (1992), 235–254.

[7] ———, *Electromagnetic considerations for RF current density imaging*, IEEE Trans. Med. Imag. **14** (1995), 515–524.

[8] E. J. Woo, S. Y. Lee, and C. W. Mun, *Impedance tomography using internal current density distribution measured by nuclear magnetic resonance*, SPIE **2299** (1994), 377–385.

Ohin Kwon
Department of Mathematics and Natural Science Research Institute
Yonsei University
Seoul 120-749, Korea
E-mail: oikwon@math.snu.ac.kr

Jin Keun Seo
Department of Mathematics
Yonsei University
Seoul 120-749, Korea
E-mail: seoj@bubble.yonsei.ac.kr

Eung Je Woo
School of Electronics and Information
Kyung Hee University
Kyungki 449-701, Korea
E-mail: ejwoo@khu.ac.kr

Jeong-Rock Yoon
School of Mathematics
Korea Institute for Advanced Study
Seoul 130-012, Korea
E-mail: jryoon@numer.kaist.ac.kr